

Cerebral glucose utilisation in hepatitis C virus infection-associated encephalopathy

Meike Heeren¹, Karin Weissenborn¹, Dimitrios Arvanitis¹, Martin Bokemeyer², Annemarie Goldbecker¹, Argyro Tountopoulou¹, Thomas Peschel³, Julian Grosskreutz^{1,4}, Hartmut Hecker⁵, Ralph Buchert⁶ and Georg Berding⁷

¹Department of Neurology, Medical School Hannover, Hannover, Germany; ²Department of Neuroradiology, Medical School Hannover, Hannover, Germany; ³Department of Psychiatry, Medical School Hannover, Hannover, Germany; ⁴Department of Neurology, University Clinic Jena, Jena, Germany; ⁵Department of Biometrics, Medical School Hannover, Hannover, Germany; ⁶Department of Nuclear Medicine, Charite-University Hospital Berlin, Berlin, Germany; ⁷Department of Nuclear Medicine, Medical School Hannover, Hannover, Germany

Patients with hepatitis C virus (HCV) infection frequently show neuropsychiatric symptoms. This study aims to help clarify the neurochemical mechanisms behind these symptoms and to add further proof to the hypothesis that HCV may affect brain function. Therefore, 15 patients who reported increasing chronic fatigue, mood alterations, and/or cognitive decline since their HCV infection underwent neurologic and neuropsychological examination, magnetic resonance imaging, ¹⁸F-fluoro-deoxy-glucose positron emission tomography of the brain, and single photon emission tomography of striatal dopamine and midbrain serotonin transporter (SERT) availability. None of the patients had liver cirrhosis. Patients' data were compared with data of age-matched controls. In addition, regression analysis was performed between cognitive deficits, and mood and fatigue scores as dependent variables, and cerebral glucose metabolism, dopamine, or SERT availability as predictors. Patients showed significant cognitive deficits, significantly decreased striatal dopamine and midbrain SERT availability, and significantly reduced glucose metabolism in the limbic association cortex, and in the frontal, parietal, and superior temporal cortices, all of which correlated with dopamine transporter availability and psychometric results. Thus, the study provides further evidence of central nervous system affection in HCV-afflicted patients with neuropsychiatric symptoms. Data indicate alteration of dopaminergic neurotransmission as a possible mechanism of cognitive decline.

Journal of Cerebral Blood Flow & Metabolism (2011) **31**, 2199–2208; doi:10.1038/jcbfm.2011.82; published online 1 June 2011

Keywords: cognitive impairment; dopamine; 5-HT; molecular imaging; positron emission tomography; single photon emission tomography

Introduction

After hepatitis C virus (HCV) had been identified as the cause of non-A and non-B hepatitis in 1989, research focussed on the impact of HCV infection on the liver. Now, more than 20 years later, it is well known from studies of the natural course of HCV infection that the development of severe liver disease is less frequent than initially feared: specifications of the lifetime prevalence of severe liver disease after HCV infection range between 0.4% and 8%

(Hoofnagle, 2002; Wiese *et al*, 2005). It also became obvious that severe chronic fatigue, which affects ~50% of the patients, is the most frequent disabling complication of HCV infection (Wiese *et al*, 2005; Poynard *et al*, 2002).

A growing number of studies have shown cognitive dysfunction besides chronic fatigue and mood alterations in HCV-infected patients with only mild liver disease (Forton *et al*, 2001, 2002; Weissenborn *et al*, 2004). There is also increasing evidence suggesting that HCV infection *per se* may result in cerebral dysfunction irrespective of the grade of liver disease and virus replication state (Weissenborn *et al*, 2006; Tillmann *et al*, 2011). The occurrence of HCV replication in the brain was shown by several groups (Forton *et al*, 2004; Wilkinson *et al*, 2009). Recently, Wilkinson *et al* (2009) provided evidence for virus replication in microglia and astrocytes.

Correspondence: Professor Dr K Weissenborn, Department of Neurology, Hannover Medical School, 30623 Hannover, Germany. E-mail: Weissenborn.Karin@mh-hannover.de

This study has no external funding.

Received 13 December 2010; revised 22 March 2011; accepted 26 April 2011; published online 1 June 2011

The aim of this study was to investigate whether cognitive dysfunction in HCV infection with mild liver disease is accompanied by distinct alterations of cerebral glucose utilisation. Considering the profile of cognitive deficits (Forton *et al*, 2002; Weissenborn *et al*, 2004), and our former results on serotonin and dopamine transporter (DAT) availability in patients with HCV infection-associated encephalopathy (Weissenborn *et al*, 2006), we hypothesised a decrease in glucose utilisation in the frontal and parietal cortices, as well as in the limbic system and a correlation between DAT availability and glucose utilisation in these regions.

Patients and methods

¹⁸F-fluoro-deoxy-glucose positron emission tomography (FDG-PET) was performed for quantitative assessment of cerebral glucose utilisation in 15 women with the characteristic neuropsychiatric syndrome of HCV infection-associated encephalopathy. The clinical manifestations of this syndrome consist of chronic fatigue, mood alterations, and deficits in attention and memory. Patients had been infected through immunoglobulin administration for anti-D prophylaxis in 1978/1979. Liver cirrhosis or severe fibrosis was excluded by liver biopsy ($n=13$) and/or by biochemical analysis (aspartate aminotransferase-to-platelet ratio index (APRI) score <1) (Wai *et al*, 2003). In all, 11 patients had been treated with interferon years ago. Five were PCR negative at the time of the study, one spontaneously and four after therapy. The genotype of the virus was 1b in all patients. Patients with a history of neurologic or psychiatric disease, concomitant disorders (including major depression), history of intravenous drugs, or current medication affecting central nervous system function were excluded.

All patients belonged to HCV patient support groups who had been informed about the study. A total of 85 group members volunteered to take part, 15 of whom were chosen randomly. There was no overlap between the patient sample of the present study and the sample in our previous report on monoaminergic neurotransmission in HCV-infected patients (Weissenborn *et al*, 2006).

Patients underwent clinical and neuropsychological examination, magnetic resonance imaging of the brain, ¹⁸F-FDG-PET, and single photon emission tomography (SPET) of mesencephalic/hypothalamic serotonin transporter (SERT) and striatal DAT availability using ¹²³I-beta-CIT (2β -carbomethoxy-3- β -(4-[¹²³I]iodophenyl)tropane).

The neuropsychological examination comprised Luria's list of words (Christensen, 1979), the Word Figure Memory Test (Weissenborn *et al*, 1996), the Recurring Figures Test (Rixecker and Hartje, 1980), the cancelling 'd' test (Brickenkamp, 1981), and the tests 'alertness', 'divided attention', 'incompatibility', 'modality comparison', 'attention shift', 'go/no go', and 'working memory' of the Testbatterie zur Aufmerksamkeitsprüfung (TAP) battery (Zimmermann and Fimm, 1989). Furthermore, the Hospital Anxiety and Depression Scale (HADS) (Zigmond and Snaith, 1983), Beck's Depression Inventory (BDI) (Beck *et al*, 1961), the FIS (Fatigue Impact Scale) (Fisk *et al*,

1994), and the Short Form-36 questionnaire (Bullinger and Kirchberger, 1998) were accomplished.

In all, 16 healthy women selected so as to match for age with patients (Table 1) served as the control group for psychometric testing. In addition, psychometric data were evaluated with regard to normative data given in the different test manuals. Single photon emission tomography results in patients were compared with historical reference data obtained from 20 healthy controls. As uptake images at 4 hours were not available in 4 controls, reference data were available from only 16 healthy controls (8 women; age 47 ± 17 years) with regard to SERT binding, but from 20 healthy controls (11 women; age 50 ± 19 years) with regard to DAT binding. Further details on reference data were given in an earlier paper (Berding *et al*, 2003).

Patients' FDG-PET data were compared with those of a control group of 12 subjects (4 women; age 47 ± 17 years) investigated with FDG-PET for suspicion of malignancy. In these subjects, first, a dynamic brain scan had been performed according to the same acquisition and reconstruction protocols as in HCV patients. Second, this additional scan for research purposes was followed by standardised whole-body scanning to localise manifestations of malignancy. Only subjects without any abnormal finding were included.

¹⁸F-FDG-PET was performed using an ECAT EXACT 922/47 system (Siemens, Erlangen, Germany). Subjects fasted for at least 6 hours before scanning. After a 10-minute transmission scan, 370 MBq ¹⁸F-FDG was injected intravenously over 30 seconds. The emission measurement was started at the start of the tracer injection. A total of 47 slices with a plane thickness of 3.4 mm were acquired in a two-dimensional mode. Both axial and transaxial resolutions of the reconstructed image (filtered back projection, Hann filter, cutoff frequency 0.4, 128×128 matrix) were 7 to 8 mm full-width at half-maximum. Attenuation correction was performed using the transmission scan data. Tissue activity concentration was measured dynamically over a period of 50 minutes (6×20 , 3×60 , 2×150 , 2×300 , 3×600 second frames). Arterialised venous blood samples were obtained as a surrogate for arterial input (Phelps *et al*, 1979). Samples of 1 mL each were collected according to the dynamic PET-measurement protocol at midframe times to obtain the tracer input function. Quantification of glucose metabolism was performed using the Gjedde-Patlak method (Gjedde, 1982; Patlak *et al*, 1983). The cerebral metabolic rate of glucose (CMR_{glc}) was calculated for each voxel within the brain using a lumped constant of 0.42. On the basis of the three-dimensional parametric map of CMR_{glc} , global CMR_{glc} was obtained as the mean value of all voxels within an isocontour at 50% of the maximum.

The CMR_{glc} maps were transformed into the anatomic standard stereotactic space according to the MNI (Montreal Neurological Institute) using the 'statistical parametric mapping' program (SPM2, Wellcome Department of Cognitive Neurology, London, UK). Transformed images were resliced to a voxel size of $2 \times 2 \times 2$ mm³. Spatial smoothing was performed using a three-dimensional isotropic Gaussian kernel of 10 mm full-width at half-maximum.

Table 1 Fatigue and depression scores

	PCR+ (n = 10)	PCR- (n = 5)	P PCR+/PCR-	P PCR-/C	P PCR+/C	Patients (P) (n = 15)	Controls (C) (n = 16)	P P/C
Age	52.6 ± 2.9	53.2 ± 4.9	0.77	0.28	0.077	52.8 ± 3.5	48.5 ± 5.9	0.06
FIS	101.8 ± 36.3	89.4 ± 51.9	0.68	0.003	0.000	97.7 ± 40.7	14.0 ± 15.0	0.000
HADS-A	10.9 ± 4.8	11.2 ± 5.6	0.95	0.004	0.000	11.0 ± 4.9	3.8 ± 2.5	0.000
HADS-D	10.0 ± 5.2	9.6 ± 6.4	0.95	0.008	0.000	9.9 ± 5.4	2.0 ± 1.8	0.000
BDI	21.4 ± 9.5	22.8 ± 15.0	0.86	0.002	0.000	21.9 ± 11.1	2.6 ± 2.3	0.000
SF36—mental	121.0 ± 78.6	165.0 ± 129.6	0.95	0.000	0.000	135.6 ± 96.1	341.9 ± 38.6	0.000
SF36—physical	118.7 ± 63.7	166.0 ± 106.7	0.77	0.003	0.000	134.4 ± 80	347.9 ± 30.7	0.000

BDI, Beck's Depression Inventory; FIS, Fatigue Impact Scale; HADS, Hospital Anxiety and Depression Scale; SF36, Short Form-36. Significance level after Bonferroni–Holm correction ($P < 0.007$). Bold values are significant.

Patients' PET data were compared with those of the control group using SPM's 'compare populations' model (two-sample *t*-test, uncorrected $P < 0.001$ on voxel level). Absolute values of CMR_{glc} were compared, i.e., no scaling was performed.

Voxel-by-voxel linear regression analysis was performed to assess correlation between patients' glucose utilisation (CMR_{glc}) and their psychometric test results, applying the statistical model 'covariates only' offered by SPM2. Correlations were considered significant if an uncorrected *P*-value of < 0.001 ($Z = 3.09$) was reached on the voxel level. Clusters comprising < 15 voxels were excluded. The anatomic automated labelling software package (Neuro-functional Imaging Group, Cyseron, Caen, France) was used for anatomic assignment of significant clusters.

Regression analyses were also performed using the scaled metabolic rate of glucose ($sCMR_{glc}$), which was obtained by dividing CMR_{glc} by global CMR_{glc} , voxel by voxel. Scaling increases the power for detection of regional effects by eliminating intrasubject variability of global CMR_{glc} .

Single photon emission tomography images (ECAM variable, Siemens) were obtained 4 hours after intravenous injection of 185 MBq ^{123}I - β -CIT to assess SERT availability, and 24 hours after injection to measure DAT availability (Berding *et al*, 2003).

To quantify tracer retention in DAT- and SERT-rich brain structures (caudate and putamen on either side for DAT, hypothalamus/midbrain for SERT) regions of interest (ROIs) of standardised shape and size were positioned manually over the respective structures on transaxial images. Nonspecific tracer retention was assessed using a reference region ROI over the occipital/cerebellar cortex. Region-of-interest definition has been described in detail in the study by Berding *et al* (2003). The binding potential, defined as (tracer retention in the ROI/tracer retention in the reference region) - 1, was used to characterise transporter availability in the ROI. As we did not observe regionally pronounced reduction in striatal DAT availability in patients, the binding potential was averaged over all four subregions for further analyses.

^{123}I - β -CIT was injected 1 day before PET scanning and 24-hour single-photon emission computed tomography images were obtained just before FDG application.

All procedures were in agreement with the corresponding guidelines of the European Association of Nuclear Medicine (Bartenstein *et al*, 2002; Tatsch *et al*, 2002).

For exclusion of cerebral lesions, conventional transverse and coronal T1-weighted magnetic resonance images (repetition time 500 milliseconds/echo time 15 milliseconds) and sagittal T2-weighted fast inversion-recovery (IR) images (repetition time 4,000 milliseconds/echo time 40 milliseconds/inversion time (TI) 130 milliseconds) of the brain were acquired using a 1.5-T GE Signa Horizon (General Electric Company, Milwaukee, WI, USA).

The study was approved by the local ethics committee and the Federal Office for Radiation Protection. Patients gave written informed consent.

Statistical Analysis

Psychometric and SPET results were first compared between PCR-positive (PCR+) patients, PCR-negative (PCR-) patients, and the corresponding controls using the Kruskal–Wallis test and, in case of a significant group effect, Mann–Whitney tests of all pairwise combinations of the three groups. This resulted in significant group differences only between patients and controls, whereas the two patient groups did not differ significantly in any of the tested variables. Therefore, both patient groups were compiled into one group, which was then compared with controls, again using the Mann–Whitney test. A (global) significance value $\alpha = 0.05$ was used. The Bonferroni–Holm procedure was applied to control for multiple testing separately for (1) age, fatigue, and depression scores ($n = 7$ variables, Table 1), (2) attention scores ($n = 21$, Table 2a), and (3) memory scores ($n = 8$ variables, Table 2b).

A pairwise Pearson's correlation analysis was performed to test for a relationship between the attention test sum score and mood and fatigue scores.

The PET data analysis was performed using the 'compare populations' and the 'Covariates only' model of the SPM2 program (Wellcome Department of Cognitive Neurology) as described above.

Results

Neuropsychological Test Results

Patients and controls did not differ significantly with regard to age and education (Table 1). However, there was a highly significant difference with regard to the

Table 2a Attention test results

	PCR+	PCR	P PCR+/PCR-	P PCR-/C	P PCR+/C	Patients	Controls	P P/C
D2 errors	6.1 ± 4.1	7.9 ± 5.5	0.679	0.168	0.495	6.7 ± 4.5	4.4 ± 3.1	0.233
D2 items	282.7 ± 58.8	266.0 ± 68.0	0.594	0.002	0.000	277.1 ± 60.1	388.8 ± 66.8	0.000
Attention shift RT sec	1,205.4 ± 778.5	1,076.5 ± 133.3	0.679	0.011	0.023	1,162.4 ± 631.4	787.1 ± 201.7	0.003
Attention shift errors	3.8 ± 3.9	3.0 ± 1.9	0.953	0.240	0.241	3.5 ± 3.3	1.9 ± 2.2	0.140
Intermodal comparison RT	732.6 ± 387.1	651.6 ± 324.6	0.679	0.004	0.000	705.6 ± 357.7	427.9 ± 51.2	0.000
Intermodal comparison misses	4.0 ± 5.4	2.8 ± 3.8	0.859	0.179	0.060	3.6 ± 4.9	0.3 ± 0.5	0.041
Intermodal comparison errors	3.8 ± 6.7	3.0 ± 2.8	0.859	0.179	0.165	3.5 ± 5.6	0.7 ± 1.0	0.089
Incompatibility RT sec	716.2 ± 407.9	565.5 ± 53.3	0.768	0.006	0.009	665.9 ± 336.5	454.8 ± 62.9	0.001
Incompatibility errors	5.4 ± 4.2	10.2 ± 13.9	0.859	0.179	0.027	7.0 ± 8.5	1.9 ± 1.9	0.019
Go/NoGo RT sec	518.6 ± 92.0	493.9 ± 70.4	0.768	0.313	0.135	510.4 ± 83.7	468.8 ± 113.6	0.101
Go/NoGo errors	0.6 ± 1.3	2.4 ± 1.5	0.019	0.040	0.698	1.2 ± 1.6	0.9 ± 1.7	0.520
Go/NoGo misses	0.6 ± 1.0	0.8 ± 1.3	0.953	0.354	0.241	0.7 ± 1.1	0.1 ± 0.3	0.175
Div. attention RT sec	765.7 ± 94.1	742.5 ± 84.1	0.859	0.660	0.165	757.9 ± 88.6	705.9 ± 63.5	0.202
Div. attention errors	4.1 ± 3.0	3.4 ± 3.7	0.513	0.905	0.220	3.9 ± 3.1	3.6 ± 4.7	0.338
Div. attention misses	5.8 ± 4.6	8.8 ± 7.0	0.513	0.032	0.036	6.8 ± 5.4	2.6 ± 2.0	0.008
Alertness RT sec	423.7 ± 148.8	410.8 ± 222.7	0.768	0.011	0.000	419.4 ± 168.6	266.6 ± 29.0	0.000
Phasic alertness	0.16 ± 0.21	0.01 ± 0.09	0.254	0.495	0.165	0.1 ± 0.2	0.04 ± 0.08	0.495
Working memory RT	741.2 ± 238.3	807.7 ± 148.0	0.371	0.006	0.068	763.3 ± 209.4	594.0 ± 122.6	0.007
Working memory errors	2.5 ± 1.9	5.0 ± 3.7	0.206	0.109	0.452	3.3 ± 2.8	2.0 ± 2.2	0.175
Working memory misses	4.7 ± 3.9	2.6 ± 0.9	0.594	0.006	0.002	4.0 ± 3.3	0.8 ± 1.6	0.000
Attention test sum score	0.44 ± 0.19	0.46 ± 0.12	0.859	0.001	0.001	0.44 ± 0.16	0.19 ± 0.12	0.000

Div, divided; RT, reaction time.

Significance level according to Bonferroni-Holm ($P < 0.002$).

Bold values are significant.

Table 2b Memory test results

	PCR+	PCR-	P PCR+/PCR-	Patients	Controls	P P/C
Luria run 1-5	36.9 ± 6.2	39.2 ± 5.4	0.086	37.7 ± 5.8	43.3 ± 4.3	0.0008
Luria run 6/5	0.83 ± 0.18	0.66 ± 0.18	0.086	0.77 ± 0.19	0.90 ± 0.11	0.05
WFMT words z	-0.14 ± 1.31	-0.12 ± 0.57	0.902	-0.13 ± 1.09	0.64 ± 1.24	0.12
WFMT figures z	-0.14 ± 1.29	0.49 ± 0.82	0.270	0.07 ± 1.16	0.54 ± 1.06	0.25
WFMT abstract items z	-0.99 ± 1.44	0.60 ± 0.75	0.462	0.14 ± 1.27	0.85 ± 0.97	0.21
WFMT concrete items z	-0.18 ± 1.18	-0.14 ± 0.34	0.999	-0.17 ± 0.96	0.40 ± 1.16	0.09
Recurring figures geometrical percentile	70.8 ± 23.4	82.2 ± 26.3	0.391	74.6 ± 24.1	84.7 ± 20.9	0.06
Recurring figures nonsense percentile	56.1 ± 27.4	37.2 ± 32.7	0.178	49.8 ± 29.5	71.1 ± 31.4	0.04

WFMT, Word Figure Memory Test.

Significance level according to Bonferroni-Holm ($P < 0.006$).

Bold values are significant.

FIS, the depression scores, and the Short Form-36 scores (Table 1).

With regard to attention scores, patients differed significantly from controls in the cancelling d test (D2 items), the reaction time (RT) in the 'modality comparison', the 'incompatibility' and the 'alertness' tests, as well as in the number of misses in the 'working memory' test. To characterise each subjects' individual attention ability by one single parameter, the fraction of the individual's pathologic results over all attention tests was used (denoted as attention test sum score). This score differed significantly between patients and controls (Table 2a).

From the memory tests, only the sum score of Luria's list of words (run 1 to 5) differed significantly between patients and controls (Table 2b).

The attention test sum score was not significantly correlated with either BDI ($P = 0.12$) or HADS scores (D: $P = 0.14$; A: $P = 0.19$). Its correlation with the fatigue score also fell just short above the level of significance ($P = 0.07$).

Single Photon Emission Tomography Results

The availability of SERT and DAT was significantly reduced in patients than in controls, whereas there was no significant difference between patient subgroups (Supplementary Appendix Figure e-1). In the entire patient group, SERT availability was 2.69 ± 0.33 compared with 3.02 ± 0.29 in controls ($P = 0.006$). The mean DAT availability was 8.11 ± 1.48 in patients compared with 9.39 ± 1.26 in controls ($P = 0.009$) (Supplementary Appendix Figures e-4 and e-5).

Positron Emission Tomography Results

Mean global CMR_{glc} did not differ between the two patient subgroups (PCR+: $0.354 \pm 0.032 \mu\text{mol/mL per min}$; PCR-: $0.356 \pm 0.057 \mu\text{mol/mL per min}$; $P = 0.91$) nor between the entire patient group and controls (patients: $0.354 \pm 0.040 \mu\text{mol/mL per min}$; controls:

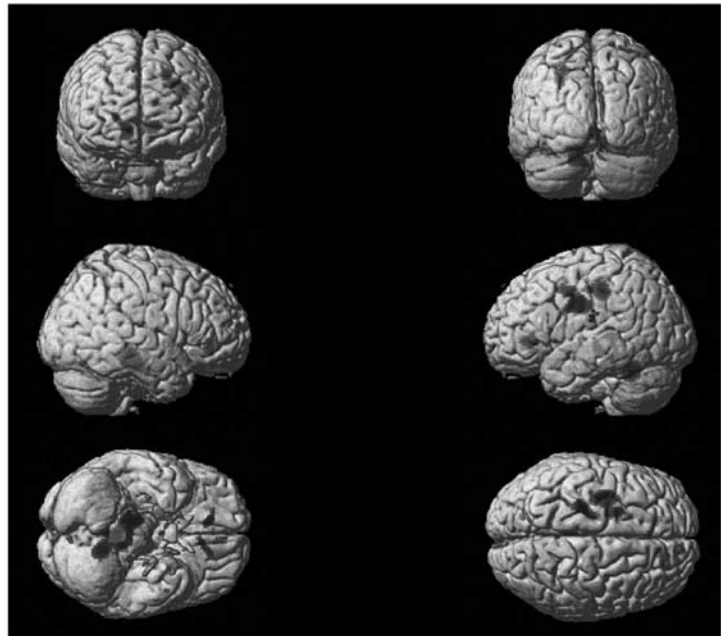
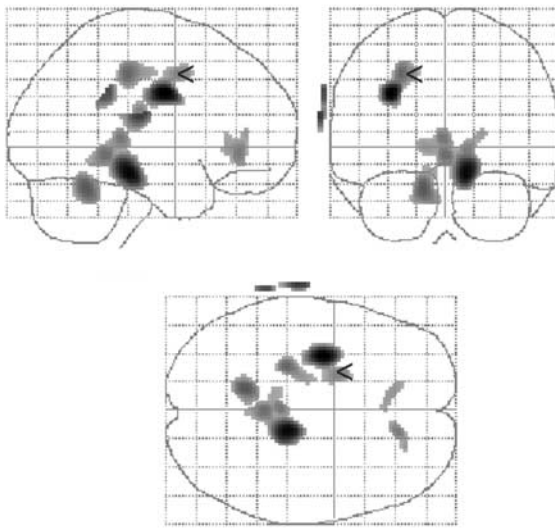


Figure 1 Cerebral glucose utilisation in HCV-associated encephalopathy. CMR_{glc} is significantly decreased in the superior and medial frontal gyri, the anterior cingulate gyrus, the hippocampus and parahippocampal gyrus, and part of the cerebellum in patients compared with controls. For statistical details, see the ‘Results’ section. CMR_{glc} , cerebral metabolic rate of glucose; HCV, hepatitis C virus.

Table 3 Regions with significantly decreased CMR_{glc} in patients compared with controls

<i>MNI coordinates</i>			<i>Cluster level k</i>	<i>Uncorrected P</i>	<i>Voxel level Z</i>	<i>Region</i>
<i>x</i>	<i>y</i>	<i>z</i>				
-32	-6	32	1,022	0.035	4.46	Gyrus frontalis superior Gyrus frontalis medius Gyrus precentralis
12	-28	-16	1,554	0.012	4.4	Vermis 4, 5 Vermis 3 Gyrus lingualis Cerebellum 4,5 Cerebellum 3 Gyrus parahippocampalis Hippocampus
-12	-52	-24	352	0.193	3.73	Cerebellum 4, 5 Cerebellum 6 Cerebellum 9
12	38	0	19	0.79	3.25	Gyrus cinguli anterior Gyrus frontalis medius, pars orbitalis

CMR_{glc} , cerebral metabolic rate of glucose; MNI, Montreal Neurological Institute.

$0.385 \pm 0.049 \mu\text{mol/mL}$ per min; $P=0.088$). The ‘compare populations’ model of SPM2 revealed significant regional effects in CMR_{glc} : CMR_{glc} was significantly reduced in patients in the superior and medial frontal gyri, the anterior cingulate gyrus, the hippocampus and parahippocampal gyrus, and part of the cerebellum (Figure 1, Table 3).

Cerebral Metabolic Rate of Glucose Versus Attention Test Results: Regression analysis revealed a negative correlation between the percentage of errors in the cancelling d test and CMR_{glc} in the median part of the

superior frontal gyrus on the right (cluster size $k=88$ voxels, maximum $Z=3.75$). The number of misses in the working memory test was negatively correlated with CMR_{glc} in the left cerebellum ($k=45$, $Z=3.51$). The RT in the modality comparison test was negatively correlated with glucose utilisation of the left cerebellum ($k>300$; $Z=3.86$), and the median cingulum ($k=171$, $Z=3.56$), the caudate nucleus ($k=36$, $Z=3.39$), and the middle frontal and the postcentral gyri on the right. The RT in the ‘alertness’ and ‘incompatibility’ tests did not show any significant correlation with regional CMR_{glc} .

Table 4 Regions with significant positive correlation between CMR_{glc} and the Luria sum score in patients

MNI coordinates			Cluster level <i>k</i>	Uncorrected <i>P</i>	Voxel level <i>Z</i>	Region
<i>x</i>	<i>y</i>	<i>z</i>				
14	-28	52	190	0.115	3.7	Gyrus cinguli medius Supplementary motor cortex Lobulus paracentralis
8	-74	-44	43	0.448	3.43	Cerebellum 7b Cerebellum 8 Vermis 8 Cerebellum Crus 2
-32	-26	44	90	0.269	3.42	Gyrus postcentralis
-30	-76	-36	33	0.51	3.36	Cerebellum Crus 2 Cerebellum Crus 1
10	32	28	46	0.432	3.33	Gyrus cinguli anterior Gyrus cinguli medius
-12	-16	60	20	0.618	3.27	Lobulus paracentralis Supplementary motor cortex
34	14	28	19	0.628	3.24	Gyrus frontalis inferior, pars triangularis Gyrus frontalis inferior, pars opercularis

CMR_{glc} , cerebral metabolic rate of glucose; MNI, Montreal Neurological Institute.

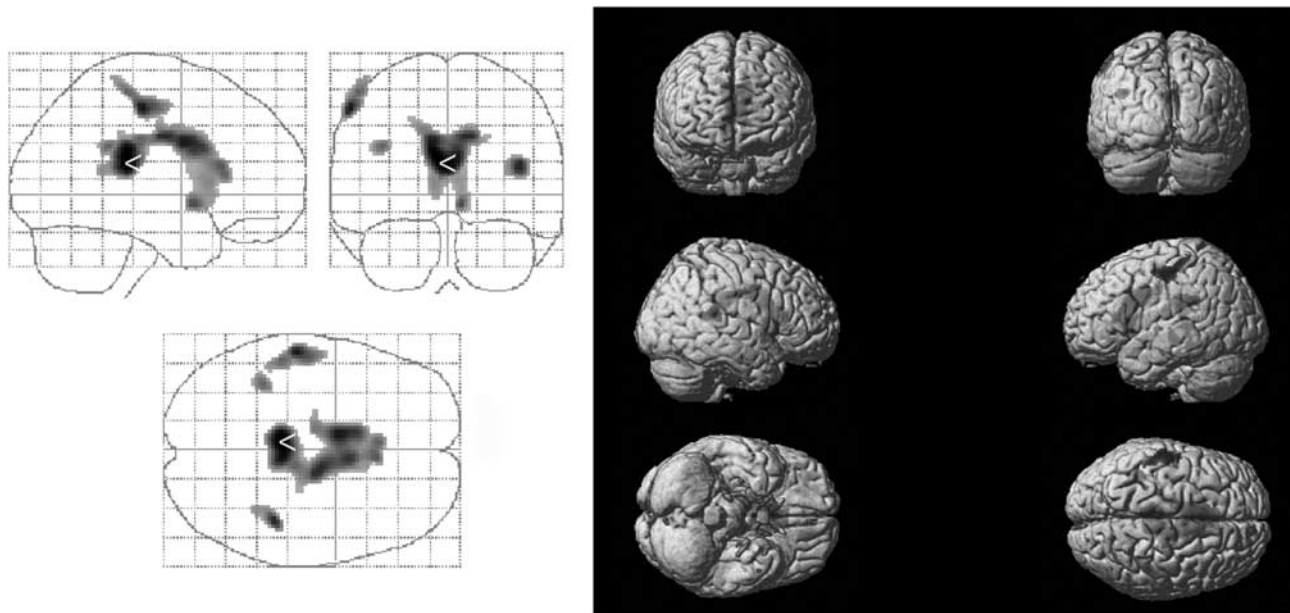


Figure 2 Memory function in HCV-associated encephalopathy: Voxels showing a significant positive correlation between CMR_{glc} and the Luria quotient as a representative of the subjects' free recall performance were located in the anterior and medial cingulate gyri and the caudate nucleus, respectively, bilaterally, the superior temporal gyrus bilaterally, the olfactory cortex, parahippocampal gyrus, amygdala, and insula on the right, the calcarine sulcus and precuneus bilaterally, and the cerebellum on the left side. For statistical details, see the 'Results' section. CMR_{glc} , cerebral metabolic rate of glucose; HCV, hepatitis C virus.

Considering scaled glucose utilisation $sCMR_{glc}$, the RT in the alertness test was negatively correlated with $sCMR_{glc}$ of all three frontal gyri and the precentral gyrus on the right, RT in the incompatibility test was negatively correlated with $sCMR_{glc}$ in the right medial frontal gyrus, and RT in the attention shift test with $sCMR_{glc}$ in the posterior cingulate gyrus on the right.

Cerebral Metabolic Rate of Glucose Versus Memory Test Results: The sum of words recalled in runs 1 to 5

of Luria's list of words test correlated significantly with CMR_{glc} in the anterior and medial cingulate gyri, the central cortex, the supplementary motor cortex, the inferior frontal gyrus, and the cerebellum (Table 4).

The quotient between the recall run 6 and the result of run 5 correlated significantly with glucose metabolism of the anterior and medial cingulate gyri and the caudate nucleus, respectively, bilaterally ($k=5,940$, $Z=5.35$), the superior temporal gyrus bilaterally, the olfactory cortex, parahippocampal

gyrus, amygdala, and insula on the right ($k=136$, $Z=4.12$), the calcarine sulcus and precuneus bilaterally, and the cerebellum on the left side (Figure 2).

Cerebral Metabolic Rate of Glucose Versus Fatigue and Depression Scores: The FIS score did not significantly correlate with CMR_{glc} but with $sCMR_{glc}$ in the caudate nucleus, the thalamus, the postcentral gyrus, the anterior and medial cingulate gyri, and particularly the orbital part of the three frontal gyri: gyrus frontalis superior, medius, and inferior bilaterally (Supplementary Appendix Table e-1, Supplementary Appendix Figure e-2). Regression analysis between CMR_{glc} and depression scores showed significant correlations also predominantly for the scaled data.

The BDI correlated negatively with $sCMR_{glc}$ of the orbitofrontal cortex and the cerebellum. The HADS-D scores correlated negatively with $sCMR_{glc}$ in the caudate, the anterior cingulate gyrus, the orbitofrontal gyri on the right, and the postcentral gyrus on the left. A positive correlation was observed for both scores with $sCMR_{glc}$ of the central region (gyrus precentralis and postcentralis). The HADS-A score correlated predominantly with $sCMR_{glc}$ of the parahippocampal gyrus and the caudate (Supplementary Appendix Tables e-2 and e-3).

Cerebral Metabolic Rate of Glucose Versus Single Photon Emission Tomography Results: Regression analysis revealed a positive correlation between the striatal DAT-binding capacity and CMR_{glc} in the

inferior and superior parietal and postcentral gyri, bilaterally, the precentral gyrus on the left, the medial cingulate gyrus bilaterally, the superior, medial, and inferior frontal gyri bilaterally, the superior temporal gyrus bilaterally, the medial temporal gyrus on the left, the temporal pole on the left, central operculum on the left, insula, putamen, and pallidum, precuneus, cuneus, and calcarine cortex bilaterally (Figure 3, Supplementary Table e-4). The SERT availability did not correlate with CMR_{glc} .

Discussion

The new concept of HCV infection-associated encephalopathy has been supported by neuroimaging findings such as detection of altered magnetic resonance spectra or proof of altered midbrain SERT—and striatal DAT availability in HCV-afflicted patients with normal liver function but neuropsychiatric symptoms (Forton *et al*, 2001, 2008; Weissenborn *et al*, 2004, 2006; McAndrews *et al*, 2005; Bokemeyer *et al*, 2011).

This study provides further evidence. A total of 15 patients, who had been infected with HCV by application of HCV-contaminated immunoglobulines ~28 years ago, and who had noticed increasing fatigue and attention, concentration, and memory deficits over the years were studied compared with healthy controls of comparable age. Importantly, there was no difference between PCR+ and PCR– patients with regard to their neuropsychiatric symptoms.

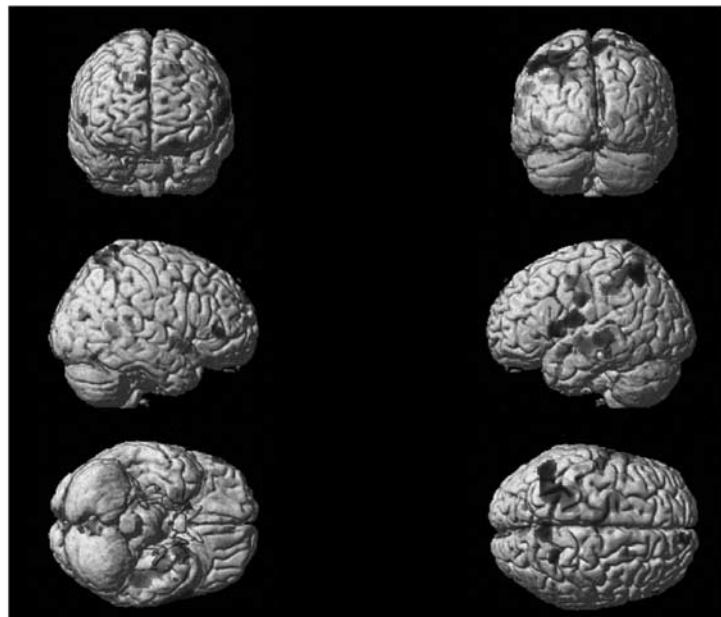
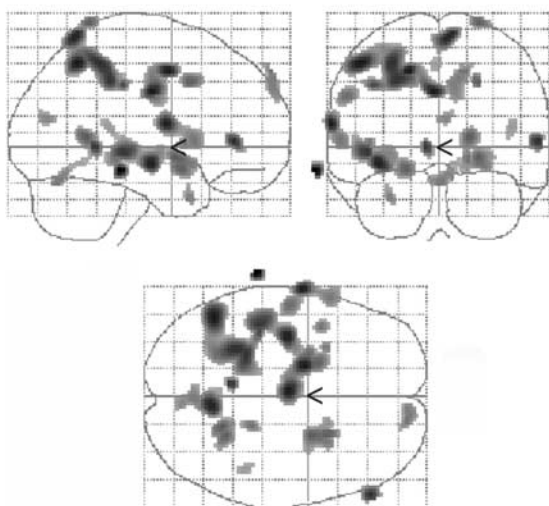


Figure 3 The dopamine system and cognition in HCV-associated encephalopathy: Voxels showing a significant positive correlation between striatal DAT availability and CMR_{glc} are located in the inferior and superior parietal and postcentral gyri, bilaterally, the precentral gyrus on the left, the medial cingulate gyrus bilaterally, the superior, medial, and inferior frontal gyri bilaterally, the superior temporal gyrus bilaterally, the medial temporal gyrus on the left, the temporal pole on the left, central operculum on the left, and insula, putamen, and pallidum, precuneus, cuneus, and calcarine cortex bilaterally. Details are given in Supplementary Table e-4. CMR_{glc} , cerebral metabolic rate of glucose; DAT, dopamine transporter; HCV, hepatitis C virus.

This finding is in line with our recent study on health-related quality of life in patients with different liver diseases, in which we observed that sustained responders may be even more affected than nonresponders to antiviral therapy (Tillmann *et al*, 2011). None of the patients included in this study had developed clinically relevant liver disease. In addition, none of the patients had any concomitant disorder affecting central nervous system function or drug addiction. Thus, the data are not biased by associated risks and epidemiologic differences between drug-abusing populations and controls, for example.

Patients differed significantly from controls with regard to their glucose utilisation at rest in the superior and medial frontal gyri, the anterior cingulate gyrus, the hippocampus and parahippocampal gyri, and part of the cerebellum. Glucose utilisation especially in the limbic association cortex, and the frontal, parietal and superior temporal cortices correlated significantly with patients' performance in attention and memory tests and with the DAT binding potential. We hypothesise that the observed changes in metabolism and neurotransmission are caused either directly or indirectly (by inflammatory mediators) by HCV infection and are the basis of clinical symptoms.

The PET findings are well in line with patients' complaints and the psychometric data showing reduced attention and memory functions. The superior and medial frontal gyri, the anterior cingulate gyrus, the hippocampus and parahippocampal gyri, which all showed a reduced glucose utilisation in patients belong to the limbic association cortex and are significantly involved in attention and memory processing. The correlation analysis showed alterations of glucose utilisation especially in regions supposed to harbour those attention processes which are predominantly altered in patients with HCV infection-associated encephalopathy. Proper function of the right frontal and parietal cortices, for example, is mandatory for normal vigilance and alertness (Fernandez-Duque and Posner, 2001). Accordingly, we found a decrease in glucose utilisation in the orbitofrontal cortex and the parietal cortex on the right with worsening performance in both the cancelling d test and the alertness test. The 'incompatibility test' and the 'modality comparison test' demand a specific reaction after proper evaluation of a stimulus, either inhibition of an automatic response (incompatibility test) or initiation of a wilful response (modality comparison test). These tasks involve the executive attention system, which is associated with the anterior cingulate gyrus, supplementary motor area, orbitofrontal cortex, and dorsolateral prefrontal cortex, part of the basal ganglia (corticostriatal loops) and the thalamus, especially on the right (Fernandez-Duque and Posner, 2001). In agreement with this, we found a correlation between the RT in the incompatibility and the modality comparison tests with glucose utilisation of several components of the executive attention system.

The attention shift test is a so-called orienting task which is believed to be performed in the parietal cortex (Fernandez-Duque and Posner, 2001). Interestingly, we found a correlation between the number of errors in the attention shift test and regional glucose metabolism in the parietal cortex on the right.

In memory tests, HCV patients performed only slightly worse than controls. After Bonferroni-Holm correction, only the Luria test results differed significantly between patients and controls. Luria's list of words (Christensen, 1979) is a short-term memory and learning test. The sum of the number of words learned in the single runs is considered to represent the subjects' learning capacity. After a 10-minute interval, the subject is asked to remember the words learned before. The quotient between the recall run (run 6) and the result of run 5 is considered to represent the subjects' incidental free recall performance for words. The correlation between the Luria sum score and CMR_{glc} indicates that the patients' learning aptitude may be impaired as a consequence of an altered function of the frontal executive attention system (Blumenfeld and Ranganath, 2007; Calabrese and Markowitsch, 2003). The free recall performance of patients significantly correlated not only with glucose utilisation of the cingulate gyrus but also with that of the amygdala and parahippocampal gyrus and the superior temporal gyrus, thus indicating an impaired function of the executive attention system and the frontotemporal structures involved in memory encoding and retrieval.

According to the sum scores of the HADS and BDI, some patients were mildly or even severely depressed, although both current and history of major depression were excluded. This is in agreement with the findings of Golden *et al* (2007) who have recently shown that BDI and HADS scores poorly correlate with Diagnostic and Statistical Manual of Mental Disorders-IV diagnosis of depression in patients with HCV. Increased variability of BDI and HADS in HCV patients might explain the lack of statistically significant correlation between CMR_{glc} and these scores. A correlation was only found after reduction of intersubject variation in CMR_{glc} by scaling to the global CMR_{glc} . Scaled CMR_{glc} showed a significant correlation with depression scores in some areas, which have been shown to be affected in depression in former studies: the orbitofrontal cortex, the cingulate gyrus, and the hippocampal region (Gupta *et al*, 2004; Kimbrell *et al*, 2002). It should be noted that scaling of CMR_{glc} to global CMR_{glc} can result in scaling artefacts as described for example in the study by Borghammer *et al* (2008). In this study, potential scaling artefacts are expected to be small, because there was only a small difference in global CMR_{glc} between the patient group and controls (not statistically significant). However, scaling artefacts cannot be ruled out. Therefore, the additional regression analyses with scaled CMR_{glc} instead of absolute CMR_{glc} are to be considered supplementary explorative analyses.

Data on cerebral glucose utilisation in patients with chronic fatigue syndrome are sparse. Tirelli *et al* (1998), in a ROI-based approach, observed hypometabolism in the right mediofrontal cortex and the brainstem. Siessmeier *et al* (2003) used an observer-independent analysis and found hypometabolism bilaterally in the cingulate gyrus and the adjacent cortical areas, as well as in the orbitofrontal cortex. There was a significant correlation between HADS and sCMR_{glc} in the cingulate gyrus, the medial and superior frontal gyri, and the parahippocampal gyrus, in good agreement with the present findings. However, Siessmeier *et al* did not find a significant correlation between cerebral glucose utilisation and the fatigue score.

As in our former study (Weissenborn *et al*, 2006), we found a significantly decreased availability of DAT and SERT in patients compared with controls. Although reduction of DAT and SERT density might be the most likely explanation for this finding, other factors including increased competition with endogenous ligands or reduced affinity of the binding site for the tracer cannot be ruled out. The significant correlation between striatal DAT availability and cerebral glucose utilisation in this study shows that cerebral dysfunction in HCV-afflicted patients is associated with alterations of dopaminergic neurotransmission. In particular, HCV-related hypometabolism in the frontal lobe might be caused by impaired mesotelencephalic dopamine projections. Dopamine neurotransmission in the prefrontal cortex is known to mediate working memory and executive functions, whereas in the parietal cortex, dopamine is known to mediate orienting reactions (Fernandez-Duque and Posner, 2001). Of interest, the pattern of regional hypometabolism including parietotemporal and frontal regions in particular, appears to be similar to that observed in Parkinson's disease (Borghammer *et al*, 2010).

In summary, this study provides further evidence for central nervous system affection in HCV-afflicted patients with neuropsychiatric symptoms. The significant correlation of cognitive performance and cerebral glucose metabolism with DAT availability provides a rationale for further studies on the role of dopaminergic neurotransmission in HCV-related neuropsychiatric impairment, particularly on dopamine receptor agonists as a therapeutic option. Finding a therapeutic option is mandatory as the neuropsychiatric symptoms that occur in about half of the HCV-afflicted patients significantly impair the patients' quality of life, and may destroy the patients' daily living abilities as well as their family life. The impact of the disorder becomes clear considering the fact that today ~9 million people in Europe and ~130 to 170 million people worldwide are estimated to be infected with HCV (Lavanchy, 2009).

Disclosure/conflict of interest

The authors declare no conflict of interest.

References

- Bartenstein P, Asenbaum S, Catafau A, Halldin C, Pilowski L, Pupi A, Tatsch K (2002) European Association of Nuclear Medicine Procedure Guidelines for Brain Imaging Using [¹⁸F]FDG. *Eur J Nucl Med Mol Imaging* 29:BP43–8
- Beck AT, Ward CH, Mendelson M, Mock JE, Erbaugh JK (1961) An inventory for measuring depression. *Arch Gen Psychiatry* 4:561–71
- Berding G, Brucke T, Odin P, Brooks DJ, Kolbe H, Gielow P, Harke H, Knoop BO, Dengler R, Knapp WH (2003) [¹²³I]beta-CIT SPECT imaging of dopamine and serotonin transporters in Parkinson's disease and multiple system atrophy. *Nuklearmedizin* 42:31–8
- Blumenfeld RS, Ranganath C (2007) Prefrontal cortex and long-term memory encoding: an integrative review of findings from neuropsychology and neuroimaging. *Neuroscientist* 13:280–91
- Bokemeyer M, Ding XQ, Goldbecker A, Raab P, Heeren M, Arvanitis D, Tillmann HL, Lanfermann H, Weissenborn K (2011) Evidence for neuroinflammation and neuroprotection in HCV infection-associated encephalopathy. *Gut* 60:370–7
- Borghammer P, Chakravarty M, Jonsdottir KY, Sato N, Matsuda H, Ito K, Arahata Y, Kato T, Gjedde A (2010) Cortical hypometabolism and hypoperfusion in Parkinson's disease is extensive: probably even at early disease stages. *Brain Struct Funct* 214:303–17
- Borghammer P, Jonsdottir KY, Cumming P, Ostergaard K, Vang K, Ashkanian M, Vafaei M, Iversen P, Gjedde A (2008) Normalization in PET group comparison studies—the importance of a valid reference region. *Neuroimage* 40:529–40
- Brickenkamp R (1981) *Test d2. Aufmerksamkeits-Belastungs-Test*. Göttingen-Toronto-Zürich: Verlag für Psychologie J. Hogrefe
- Bullinger M, Kirchberger I (1998) *Der SF-36 Fragebogen zum Gesundheitszustand (SF-36) Handbuch Für Die Deutschsprachige Fragebogenversion*. Hogrefe—Verlag für Psychologie: Göttingen, Bern, Toronto, Seattle
- Calabrese P, Markowitsch HJ (2003) Gedächtnis und Gehirn—Neurobiologische Korrelate von Gedächtnisstörungen. *Fortschr Neurol Psychiat* 71:211–9
- Christensen AL (1979) *Luria's Neuropsychological Investigation*. Text (2nd edn). Munksgaard: Copenhagen
- Fernandez-Duque D, Posner MI (2001) Brain imaging of attentional networks in normal and pathological states. *J Clin Exp Neuropsychol* 23:74–93
- Fisk JD, Ritvo PG, Ross L, Haase DA, Marrie TJ, Schlech WF (1994) Measuring the functional impact of fatigue: validation of the fatigue impact scale. *Clin Infect Dis* 18(Suppl 1):S79–83
- Forton DM, Allsop JM, Main J, Foster GR, Thomas HC, Taylor-Robinson SD (2001) Evidence for a cerebral effect of the hepatitis C virus. *Lancet* 358:38–9
- Forton DM, Thomas HC, Murphy CA, Allsop JM, Foster GR, Main J, Wesnes KA, Taylor-Robinson SD (2002) Hepatitis C and cognitive impairment in a cohort of patients with mild liver disease. *Hepatology* 35: 433–9
- Forton DM, Karayianni P, Mahmud N, Taylor-Robinson SD, Thomas HC (2004) Identification of unique hepatitis C virus quasispecies in the central nervous system and comparative analysis of internal translational efficiency of brain, liver, and serum variants. *J Virol* 78:5170–83

- Forton DM, Hamilton G, Allsop JM, Grover VP, Wesnes K, O'Sullivan C, Thomas HC, Taylor-Robinson SD (2008) Cerebral immune activation in chronic hepatitis C infection: a magnetic resonance spectroscopy study. *J Hepatol* 49:316–22
- Gjedde A (1982) Calculation of glucose phosphorylation from brain uptake of glucose analogs *in vivo*: a re-examination. *Brain Res Rev* 4:237–74
- Golden J, Conroy RM, O'Dwyer AM (2007) Reliability and validity of the Hospital Anxiety and Depression Scale and the Beck Depression Inventory (Full and Fast Screen Scales) in detecting depression in persons with hepatitis C. *J Affect Dis* 100:265–9
- Gupta A, Elheis M, Pansari K (2004) Imaging in psychiatric illnesses. *Int J Clin Pract* 58:850–8
- Hoofnagle JH (2002) Course and outcome of hepatitis C. *Hepatology* 36:S21–9
- Kimbrell TA, Ketter TA, George MS, Little JT, Benson BE, Willis MW, Herscovitch P, Post RM (2002) Regional cerebral glucose utilization in patients with a range of severities of unipolar depression. *Biol Psychiatry* 51:237–52
- Lavanchy D (2009) The global burden of hepatitis C. *Liver Int* 29(Suppl 1):74–81
- McAndrews MP, Farcnik K, Carlen P, Damyanovich A, Mrkonjic M, Jones S, Heathcote EJ (2005) Prevalence and significance of neurocognitive dysfunction in hepatitis C in the absence of correlated risk factors. *Hepatology* 41:801–8
- Patlak C, Blasberg RG, Fenstermacher JD (1983) Graphical evaluation of blood-to brain transfer constants from multiple-time uptake data. *J Cereb Blood Flow Metab* 3:1–7
- Phelps ME, Huang SC, Hoffman EJ, Selin C, Sokoloff L, Kuhl DE (1979) Tomographic measurement of local cerebral glucose metabolic rate in humans with (F-18) 2-fluoro-2-deoxy-D-glucose: validation of method. *Ann Neurol* 6:371–88
- Poynard T, Cacoub P, Ratziu V, Myers RP, Dezailles MH, Mercadier A, Ghillani P, Charlotte F, Piette JC, Moussalli J, Multivirc group (2002) Fatigue in patients with chronic hepatitis C. *J Viral Hepatitis* 9:295–303
- Rixecker H, Hartje W (1980) Kimura's recurring-figures-test: a normative study. *J Clin Psychol* 36:465–7
- Siessmeier T, Nix WA, Hardt J, Schreckenberger M, Egle UT, Bartenstein P (2003) Observer independent analysis of cerebral glucose metabolism in patients with chronic fatigue syndrome. *J Neurol Neurosurg Psychiatry* 74:922–8
- Tatsch K, Asenbaum S, Bartenstein P, Catafau A, Halldin C, Pilowsky LS, Pupi A, European Association of Nuclear Medicine (2002) European Association of Nuclear Medicine Procedure Guidelines for Brain Neurotransmission SPET Using (123)I-Labelled Dopamine Transporter Ligands. *Eur J Nucl Med Mol Imaging* 29: BP30–5
- Tillmann HL, Wiese M, Braun Y, Tenckhoff S, Mössner J, Manns MP, Weissenborn K (2011) Quality of life in patients with various liver disease. HCV patients show greater mental impairment while PBC patients have greater physical impairment. *J Viral Hep* 18: 252–61
- Tirelli U, Chierichetti F, Tavio M, Simonelli C, Bianchin G, Zanco P, Ferlin G (1998) Brain positron emission tomography (PET) in chronic fatigue syndrome: preliminary data. *Am J Med* 105:54S–8S
- Wai CT, Greenon JK, Fontana RJ, Kalbfleisch JD, Marrero JA, Conjeevaram HS (2003) A simple noninvasive index can predict both significant fibrosis and cirrhosis in patients with chronic hepatitis C. *Hepatology* 38:518–26
- Weissenborn K, Ennen JC, Bokemeyer M, Ahl B, Wurster U, Tillmann H, Trebst C, Hecker H, Berding G (2006) Monoaminergic neurotransmission is altered in hepatitis C virus infected patients with chronic fatigue and cognitive impairment. *Gut* 55:1624–30
- Weissenborn K, Krause J, Bokemeyer M, Hecker H, Schüler A, Ennen JC, Ahl B, Manns MP, Böker KW (2004) Hepatitis C virus infection affects the brain—evidence from psychometric studies and magnetic resonance spectroscopy. *J Hepatol* 41:845–51
- Weissenborn K, Rückert N, Brassel F, Becker H, Dietz H (1996) A proposed modification of the Wada test for presurgical assessment in temporal lobe epilepsy. *Neuroradiology* 38:422–9
- Wiese M, Gröngreiff K, Gühoff W, Lafrenz M, Oesen U, Porst H, for the East German Hepatitis C Study Group (2005) Outcome in a hepatitis C (genotype 1b) single source outbreak in Germany—a 25 year multicenter study. *J Hepatol* 43:590–8
- Wilkinson J, Radkowski M, Laskus T (2009) Hepatitis C virus neuroinvasion: identification of infected cells. *J Virol* 83:1312–9
- Zigmond AS, Snaith RP (1983) The Hospital Anxiety and Depression Scale. *Acta Psychiatr Scand* 67:361–70
- Zimmermann P, Fimm B (1989) *Neuropsychologische Testbatterie zur Erfassung von Aufmerksamkeitsdefiziten—Revidierte Fassung*. Freiburg: Psychologisches Institut der Universität Freiburg

Supplementary Information accompanies the paper on the Journal of Cerebral Blood Flow & Metabolism website (<http://www.nature.com/jcbfm>)